Electrochimica Acta

journal homepage: www.elsevier.com/locate/electacta

Seebeck coefficients of cells with lithium carbonate and gas electrodes

M.T. Børset[a], X. Kang[d], O.S. Burheim[c], G.M. Haarberg[b], Q. Xu[e], S. Kjelstrup[a,*]

[a] Department of Chemistry, Norwegian University of Science and Technology, NO-7491 Trondheim, Norway
[b] Department of Materials Technology and Engineering, Norwegian University of Science and Technology, NO-7491 Trondheim, Norway
[c] Faculty of Technology, Sør-Trøndelag University College, Trondheim, Norway
[d] School of Materials Science and Metallurgy, Northeastern University, Shenyang, Liaoning, 110819, China
[e] School of Materials Science and Engineering, Shanghai University, Shanghai, 200072, China

ARTICLE INFO

ABSTRACT

The Seebeck coefficient is reported for thermoelectric cells with gas electrodes and a molten electrolyte of one salt, lithium carbonate, at an average temperature of 750 °C. We show that the coefficient, which is $0.88\,\mathrm{mV\,K^{-1}}$, can be further increased by adding an inorganic oxide powder to the electrolyte. We interpret the measurements using the theory of irreversible thermodynamics and find that the increase in the Seebeck coefficient is due to a reduction in the transported entropy of the carbonate ion when adding solid particles to the alkali carbonate. Oxides of magnesium, cerium and lithium aluminate lead to a reduction in the transported entropy from 232 ± 12 to around $200 \pm 4\,\mathrm{J\,K^{-1}\,mol^{-1}}$. This is of importance for design of thermoelectric converters.

1. Introduction

Renewable energy technologies are high on the global research agenda as one of the means to meet energy security and the global warming challenge [1–3]. Thermoelectric power generators produce electricity directly from heat via the Seebeck effect. The power can be generated from various heat sources and with no moving parts. The devices are expected to take part both in primary power production and to be able to improve the overall energy efficiency of existing plants [4,5]. Most of the research activity has been concentrated on the use of semiconductors [4,6], with the aim to increase the efficiency of the thermoelectric materials itself. However, the successful deployment depends also on the cost per watt produced [7,8].

A high thermoelectric conversion efficiency, as measured by the so-called figure of merit, is obtained when the system has a high Seebeck coefficient, a low thermal conductivity and a low electrical resistivity [9]. The Seebeck coefficient is directly related to the Peltier heat, through irreversible thermodynamic theory, see e.g., Agar [10], de Groot and Mazur [11] or Førland et.al [12]. The Peltier heat is the reversible heat change at the interfaces when charge is transferred from one phase to another. Semiconductors have

Seebeck coefficients of typically $200\,\mu\mathrm{V\,K^{-1}}$, but gigantic values have been reported, e.g. $45\,\mathrm{mV\,K^{-1}}$ in strongly correlated semiconductor $\mathrm{FeSb_2}$ [13], $850\,\mu\mathrm{V\,K^{-1}}$ for a two-dimensional electron gas in $\mathrm{SrTiO_3}$ [14] and $450\,\mu\mathrm{V\,K^{-1}}$ at 900 K for $\mathrm{SrTiO_3/SrTi_{0.8}Nb_{0.2}O_3}$ superlattices [15]. In electrochemical systems, the Seebeck coefficient can be much larger, when the entropy change of the electrode reaction is large. Especially for cells involving complex formation or with gas electrodes. For example, Bonetti et.al. [16] reported a Seebeck coefficient near $7\,\mathrm{mV\,K^{-1}}$ for non-aqueous electrolytes at low temperatures (30-40 °C). For systems with ionic liquids, Abraham and co-workers reported Seebeck coefficients of 1.5-$2.2\,\mathrm{mV\,K^{-1}}$. For molten salts, Flem et.al [17] reported Seebeck coefficients up to $1.8\,\mathrm{mV\,K^{-1}}$ for oxygen electrodes in an electrolyte with molten cryolite and oxides at 960 °C. Jacobsen and Broers [18] reported values around $1.2\,\mathrm{mV\,K^{-1}}$ at 800-1150 K for equimolar mixtures of alkali carbonates and gas electrodes. Sales and co-workers explored capacitive membrane technology for thermal energy harvesting from small temperature differences [19]. There are two main reasons why we find it interesting to investigate electrochemical systems as potential thermoelectric power generators: 1) the potential for large Seebeck coefficients combined with 2) the possibility to avoid the use of toxic and rare elements. Pursuing this pathway, we aim to find a safe and potentially cheap thermoelectric power generator.

We seek electrochemical systems with higher Seebeck coefficients than semiconductors, targeting heat recovery in the metallurgical industry [20]. In this industry, heat is available at temperatures from 1600 °C and down to room temperature [21–23].

* Corresponding author.
    E-mail addresses: marit.takla.borset@ntnu.no
(M.T. Børset), kx81@163.com (X. Kang), odnesb@hist.no
(O.S. Burheim), geir.martin.haarberg@ntnu.no (G.M. Haarberg), qianxu@shu.edu.cn
(Q. Xu), signe.kjelstrup@ntnu.no (S. Kjelstrup).

We have chosen to investigate carbonates and electrodes reversible to carbonate ions as candidate systems as they are stable liquids at intermittent temperatures ($400\,^\circ$C to $800\,^\circ$C). The choice was motivated by the early results for mixtures of alkali carbonates by Jacobsen and Broers [18]. Alkali carbonates are used as electrolytes in molten carbonate fuel cells and have been studied extensively since the 1960's. Thus, for systems development, we expect to draw on this knowledge.

Here, we combine theoretical and experimental studies and start to build systematic knowledge about the Seebeck coefficient. We apply the method of irreversible thermodynamics to establish the transport equations for the system. This theory has progressed over the last few years to be able to deal with heterogeneous systems [24]. Yet, few applications of this new method have been made to thermoelectric phenomena. The transport equations give a framework that helps to define conditions that gives well defined experiments. Also, these equations gives information on temperature profiles and electric potential profiles as well as a framework suitable for optimization of a working unit. We express the Seebeck coefficient in terms of the thermodynamic entropies of the components and the transported entropies of the charge carriers. While a few models exists to explain the reversible heat effect, or the transported entropies of semiconductors, models are not available for the transported entropy of ions. Over the years, the transported entropy of an ion has most often been compared to the thermodynamic entropy of an ion. The difference between the two is the Eastman entropy. Lists have been made of single electrode heats, for one or two-component electrolytes, but we think it is fair to say that there is as of yet no detailed model able to predict the magnitude of the transported entropy.
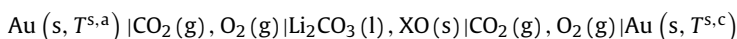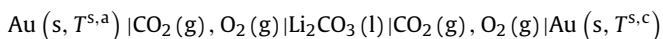
Jacobsen and Borers [18] added powder of magnesium oxide to the liquid mixtures of two or three alkali carbonates, giving a more viscous electrolyte easier to handle. We choose to start simple with a single alkali carbonate as electrolyte, pure lithium carbonate. A series of inorganic compounds is next introduced in the molten carbonate, $MgO(s)$, $CeO_2(s)$ and $LiAlO_2(s)$. The addition of a powder in the solid state does not alter the expression for the Seebeck coefficient, but it does have an impact on the value of the coefficient, caused by variations in the transported entropy of carbonate ions. The presence of $LiAlO_2(s)$, but not $CeO_2(s)$, alters the symmetry of the carbonate ion [25,26]. We use $MgO(s)$ to be able to compare with earlier results [18]. We also considered to add SiO_2, but this is was not feasible as SiO_2 greatly enhance the decomposition of lithium carbonate [27].

The paper is organized as follows. In the theoretical part, we divide the total cell into five subsystems. For each subsystem we establish the entropy production and give the flux equations that follow from this. From the flux equations, we find the contribution from the subsystems to the cell's Seebeck coefficient. Next, we report the experimental technique along with measurements that verify and confirm the reliability of the technique used. We see that the large Seebeck coefficient for the single component electrolyte can be enhanced by making use of a dispersion of particular solid inorganic oxides. The additive leads to a reduction in the transported entropy of carbonate ions.

2. Theory

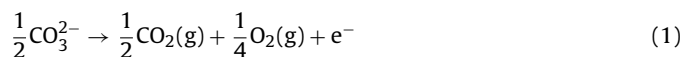### 2.1. System description

Consider the conversion of thermal energy into electric energy in two cells with electrodes reversible to the carbonate ion:

$$\mathrm{Au}\left(s, T^{s,a}\right)|CO_2(g), O_2(g)|Li_2CO_3(l)|CO_2(g), O_2(g)|\mathrm{Au}\left(s, T^{s,c}\right) \tag{LC}$$

$$\mathrm{Au}\left(s, T^{s,a}\right)|CO_2(g), O_2(g)|Li_2CO_3(l), XO(s)|CO_2(g), O_2(g)|\mathrm{Au}\left(s, T^{s,c}\right) \tag{LC-XO}$$

Here the cells labels refer to the electrolyte used, LC designate pure molten lithium carbonate while LC-XO is a dispersion of molten lithium carbonate and an oxide (XO) in the solid state, where XO represents the oxides MgO, CeO_2 or $LiAlO_2$. The cells have two carbon dioxide|oxygen electrodes, kept at temperatures $T^{s,a}$ and $T^{s,c}$. The electrode gases are bubbled over electron conductors of gold, immersed in an electrolyte of uniform composition. Jacobsen and Broers [18] used platinum electrodes, but we use gold electrodes. Both platinum and gold have proven to be stable, reproducible and reversible in molten carbonates [28]. The value of the Seebeck coefficient is not affected by the choice of electrode material, given that the electrode reaction is the same, as the transported entropy of the electron is small and negligible in both metals. We shall see below that the presence of the oxide XO in the electrolyte will have no effect on the theoretical expression of the Seebeck coefficient, but will change the value of the coefficient even if its solubility in the electrolyte is negligible. The addition of oxide could affect the solubility of the gases in the electrolyte, however, only the gas state of carbon dioxide and oxygen enters the overall electrochemical reaction. This is why cells LC and LC-XO can be used to learn about the transported entropy of the carbonate ion.

The overall electrochemical reaction at the left-hand side is [29]:

$$\frac{1}{2}CO_3^{2-} \rightarrow \frac{1}{2}CO_2(g) + \frac{1}{4}O_2(g) + e^- \tag{1}$$

while the opposite reaction takes place at the other side of the cell.

To facilitate the theoretical description, we divide cells LC and LC-XO into five subsystems, consisting of three homogeneous phases and two interfaces; the anode conductor (a), the two electrode surfaces (s,a and s,c), the electrolyte (e) and the cathode conductor (c). The symbols and notation are illustrated in Fig. 1a.

To establish the expression for the Seebeck coefficient, we need an expression for the emf measured between two Cu wires attached to the Au conductors at room temperature ($T^{a,o} = T^{a,o} = T^0$) when the two electrodes are at temperatures $T^{s,a}$ and $T^{s,c}$. The Seebeck coefficient is defined as the potential difference divided by the temperature difference between the electrodes in the limits $j \rightarrow 0$ and $T^{s,c} - T^{s,a} = \Delta T \rightarrow 0$:

$$\alpha_S \equiv \left(\frac{\Delta\phi}{\Delta T}\right)_{j\rightarrow 0, \Delta T\rightarrow 0} = \frac{\Delta_a\phi + \Delta_c\phi}{\Delta T} + \frac{\Delta_{a,e}\phi + \Delta_{e,c}\phi}{\Delta T} + \frac{\Delta_e\phi}{\Delta T} \tag{2}$$

where we used that the measured emf is the sum of the potential difference across each subsystem and that the electrodes are thermostatted, i.e. $T^{a,e} = T^{s,a} = T^{e,a}$ and $T^{e,c} = T^{s,c} = T^{c,e}$, *c.f.* Fig. 1a. We shall find an expression for $\Delta\phi$ from non-equilibrium thermodynamics theory for heterogeneous systems as outlined in [24].

2.2. Application of non-equilibrium thermodynamics

We shall evaluate the contribution from each subsystem to the cell potential, and hence the Seebeck coefficient, see Eq. (2). For each subsystem we establish the entropy production and give the flux equations that follows. From the flux equations we find the expression for the potential difference that enter the Seebeck coefficient for cells LC and LC-XO. The equations for the Au(s) conductors (a and c in Fig. 1a) have been given elsewhere (see *e.g.*, chapter 9 in [24]). The equations for the electrode surfaces (s,a and s,c) and the electrolyte (e) have not been established before.

2.2.1. The conductors connecting the cell

By integrating the expression for the electric potential from the temperature of the surroundings, T^0, to the electrode temperature
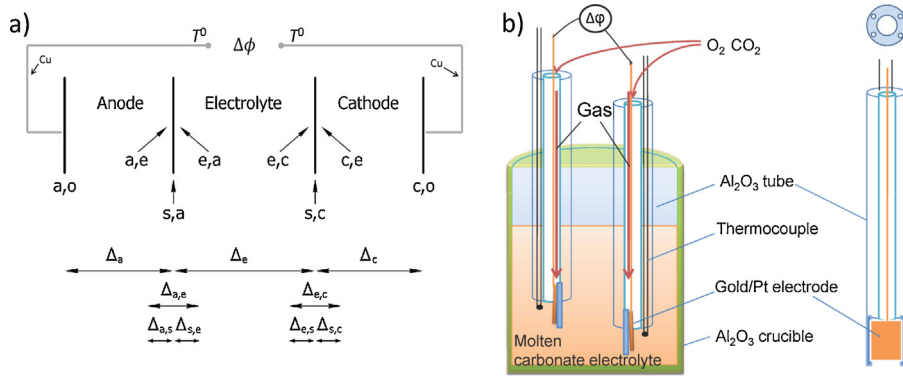
Fig. 1. A schematic picture of the cell (a) and a cross section of the experimental cell with electrodes (b). In a) we show the five subsystems of the cell and the notation used for transport properties. The first superscript refers to the phase in question, and the second to the neighboring phase. A Δ with one subscript, i, denotes the difference across phase i. A Δ with two subscripts, i, k, denotes the value in phase k minus the value in phase i. In b) we show a cross section of the cell used in the experiments. The electrodes consist of a gold wire which is point-welded to a gold plate (the electrode surface). We used a five bore Al_2CO_3 as insulation for thermocouples and electrodes, cross-section shown in the figure.

$T^{s,a}$ on the left hand-side, and from the electrode temperature on the right-hand side, $T^{s,c}$, to T^0, we find the contributions from the conductors to the Seebeck coefficient (see chapter 9 in [24]):

$$\frac{\Delta_a\phi + \Delta_c\phi}{\Delta T} = -\frac{1}{F}S_e^* \tag{3}$$

Here S_e^* is the transported entropy of the electron, this was assumed constant in the temperature interval ΔT. The origin of this expression will be explained below, in the section describing the electrolyte.

2.2.2. The electrode surfaces

The surfaces (s,a and s,c in Fig. 1a) can be regarded as independent thermodynamic systems. The thermodynamic properties of the surface are then described by excess densities, as explained *e.g.* by [24] (chapter 5). The excess entropy production in the anode surface (s,a) has contributions from heat fluxes into and out of the surface, from fluxes of oxygen and carbon dioxide out of the surface, from a flux of lithium carbonate into the surface, from the electric current density across the surface and the electrochemical reaction in the surface (see Eq. (1)):

$$\sigma^{s,a} = J_q^{\prime a,e}\Delta_{a,s}\left(\frac{1}{T}\right) + J_q^{\prime e,a}\Delta_{s,e}\left(\frac{1}{T}\right) - \frac{1}{T^{s,a}}J_{O_2}^{e,a}\Delta_{s,e}\mu_{O_2,T}\left(T^{s,a}\right)$$

$$- \frac{1}{T^{s,a}}J_{CO_2}^{e,a}\Delta_{s,e}\mu_{CO_2,T}\left(T^{s,a}\right) - \frac{1}{T^{s,a}}J_{Li_2CO_3}^{e,a}\Delta_{s,e}\mu_{Li_2CO_3,T}\left(T^{s,a}\right)$$

$$- \frac{1}{T^{s,a}}j\Delta_{a,e}\phi + r^s\left(-\frac{1}{T^{s,a}}\Delta_n G^{s,a}\right) \tag{4}$$

Here $J_q^\prime$ is the measurable heat flux and J_j is the flux of component j, $\mu_{j,T}$ is the chemical potential of component j evaluated at constant temperature T, j is the electric current density and $\Delta_{a,e}\phi$ is the potential drop across the surface. Fig. 1a gives further explanations of the notation. With thermostatted electrodes, we

have constant temperature across each surface (i.e. for s,a we have $T^{a,e} = T^{s,a} = T^{e,a}$). We assume also chemical equilibrium for adsorbed components (i.e. $\mu_j^{s,a} = \mu_j^{e,a}$). Both conditions apply to reversible conditions ($\sigma^{s,a} = 0$). We measure the emf when a very small electric current is passing the electrode, and the surface reaction rate is $r^s = j/F$. For $\sigma^{s,a} = 0$ the potential drop across the anode surface is:

$$\Delta_{a,e}\phi = -\frac{1}{F}\Delta_n G^{s,a} \tag{5}$$

Here $\Delta_n G^{s,a}$ has contributions from the neutral gas components CO_2 and O_2 to the electrode reaction:

$$\Delta_n G^{s,a} = \frac{1}{2}\mu_{CO_2}^{s,a}\left(T^{s,a}\right) + \frac{1}{4}\mu_{O_2}^{s,a}\left(T^{s,a}\right) \tag{6}$$

We introduce Eq. (6) into Eq. (5) and express the potential drop across the anode surface in terms of the chemical potentials of the neutral components:

$$\Delta_{a,e}\phi = -\frac{1}{F}\left(\frac{1}{2}\mu_{CO_2}^{s,a}\left(T^{s,a}\right) + \frac{1}{4}\mu_{O_2}^{s,a}\left(T^{s,a}\right)\right) \tag{7}$$

The same analysis applies to the other electrode surface. The total contribution from the electrode reactions to the cell potential is then:

$$\begin{aligned}\Delta_{a,e}\phi + \Delta_{e,c}\phi &= -\frac{1}{F}\left[\frac{1}{2}\left(\mu_{CO_2}^{s,a}\left(T^{s,a}\right) - \mu_{CO_2}^{s,c}\left(T^{s,c}\right)\right) + \frac{1}{4}\left(\mu_{O_2}^{s,a}\left(T^{s,a}\right) - \mu_{O_2}^{s,c}\left(T^{s,c}\right)\right)\right] \\ &= -\frac{1}{F}\left(\frac{1}{2}S_{CO_2} + \frac{1}{4}S_{O_2}\right)\left(T^{s,c} - T^{s,a}\right) \end{aligned} \tag{8}$$

We used the relation $\left(\partial\mu_j/\partial T\right)_{p,n_i} = -S_j$ to obtain the last equality. We shall evaluate S_j for the average cell temperature. The contribution from the surfaces to the Seebeck coefficient (Eq. (2)) is:

$$\frac{\Delta_{a,e}\phi + \Delta_{e,c}\phi}{\Delta T} = -\frac{1}{F}\left(\frac{1}{2}S_{CO_2} + \frac{1}{4}S_{O_2}\right) \tag{9}$$

2.2.3. One-component electrolyte

The electrolyte of cell LC is pure molten lithium carbonate and the pressure is constant throughout the system. Thus, only two thermodynamic forces contribute to the entropy production in the electrolyte (e): the thermal force and the gradient in the electric potential. The entropy production is:

$$\sigma^e = J_q^{\prime e}\left(\frac{\partial}{\partial x}\frac{1}{T}\right) + j\left(-\frac{1}{T}\frac{\partial\phi}{\partial x}\right) \tag{10}$$
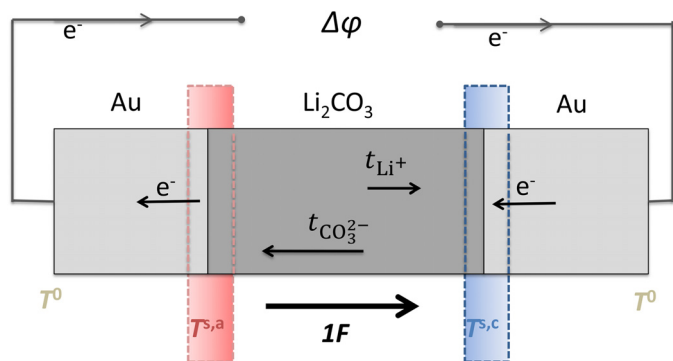
Fig. 2. The charge transport taking place in cells LC and LC–XO by transference of 1F positive charges from left to right inside the cell. The transport number t_i is the fraction of current carried by the ion i.

The flux equations for transport of heat and charge in the electrolyte follow from the entropy production:

$$J_q'^e = L_{qq}^e \left(-\frac{1}{T^2} \frac{dT}{dx} \right) + L_{q\phi}^e \left(-\frac{1}{T} \frac{d\phi}{dx} \right) \tag{11}$$

$$j = L_{\phi q}^e \left(-\frac{1}{T^2} \frac{dT}{dx} \right) + L_{\phi\phi}^e \left(-\frac{1}{T} \frac{d\phi}{dx} \right) \tag{12}$$

The coefficients (L's) depend on state variables, but are independent of the forces. They are related through the Onsager relations as $L_{q\phi} = L_{\phi q}$. The coefficients are phenomenological and must therefore be determined from experiments. We solve for $d\phi/dx$ from Eq. (12), integrate across the electrolyte for $j \approx 0$, and express the contribution from the electrolyte to the Seebeck coefficient as:

$$\frac{\Delta_e \phi}{\Delta T} = -\frac{\pi^e}{TF} \tag{13}$$

where F is Faraday's constant and we took the ratio π^e/T constant over the temperature interval. The Peltier coefficient of the electrolyte, π^e, describes the heat transported with the current at uniform temperature and composition (*i.e.* at *reversible* conditions):

$$\pi^e \equiv \left(\frac{J_q'^e}{j/F} \right)_{dT=0, d\mu_T=0}$$

$$= F \frac{L_{q\phi}}{L_{\phi\phi}} = \left(\frac{T \left(J_S^e - S_{Li_2CO_3} J_{Li_2CO_3} \right)}{j/F} \right)_{dT=0, d\mu_T=0} \tag{14}$$

where J_S^e is the entropy flux in absence of a flux of Li_2CO_3 when charge is transported in the electrolyte.

We need a more detailed expression for π^e. This can be found from the definition in Eq. (14), by considering the entropy balance of a volume element in the electrolyte at reversible conditions (isothermal conditions). To describe the movement of ions in the electrolyte(Li^+ and CO_3^{2-}) and the component (Li_2CO_3) we need a frame of reference. We follow the general procedure outlined in Ref. [30] and take either the cations or the anions as the frame of reference, *i.e.* $t_{Li^+} = 0$ or $t_{CO_3^{2-}} = 0$ (see Fig. 2). This gives two equivalent expressions for the Peltier coefficient, because both the $\Delta \phi$ and the ΔT in Eq. (13) are independent of the frame of reference. The transference coefficient of the lithium carbonate is defined as:

$$t_{Li_2CO_3} \equiv \left(\frac{J_{Li_2CO_3}}{j/F} \right)_{dT=0, d\mu_T=0} = \frac{L_{q\phi}^e}{L_{\phi\phi}^e} \tag{15}$$

In a cation frame of reference [30], the transport number of the carbonate ion is unity and the transference coefficient of the salt, $t_{Li_2CO_3} = 0$. Then, all entropy, or equivalently, heat, is transported

by the carbonate ion and the Peltier coefficient can be expressed by the transported entropy of the carbonate ion:

$$\pi^e = -T \frac{1}{2} S_{CO_3^{2-}}^* \tag{16}$$

Here the convention used for transport of charge gives the minus sign (*c.f.* Fig. 2).

In an anion frame of reference [30], the transport number of the lithium ion is unity and the transference coefficient $t_{Li_2CO_3} = 1/2$. From Eq. (15) the Peltier coefficient then equals the difference between the entropy transported with Li^+, $S_{Li^+}^*$, and the entropy transferred with Li_2CO_3:

$$\pi^e = T(S_{Li^+}^* - \frac{1}{2} S_{Li_2CO_3}) \tag{17}$$

As discussed above Eqs. (16) and (17) must be identical and we find the relation between the transported entropy of the ions and the thermodynamic entropy of the Li_2CO_3:

$$S_{CO_3^{2-}}^* + 2S_{Li^+}^* = S_{Li_2CO_3} \tag{18}$$

The relation between transported entropies and thermodynamic entropies was already shown, see *e.g.*, Agar [10], de Groot and Mazur [11] and Førland et.al [12].

2.2.4. Dispersions of lithium carbonate and an inorganic oxide

Inorganic oxides in the solid state can be added to molten lithium carbonate electrolyte, as in cell LC–XO, without altering the form of the theoretical description of the cell emf. We take MgO as an example to see that this statement is true. An equilibrium can be established between MgO(s) and CO_2(g) in the melt to give $MgCO_3$(l) according to Eq. (19)

$$MgO(s) + CO_2(g) \rightleftharpoons MgCO_3(l) \tag{19}$$

Van Velden [31] studied the equilibrium between alkali-magnesium carbonate melts, carbon dioxide gas and magnesium oxide. The mole fraction of $MgCO_3$(l) in the carbonate melt was about 0.12 at 450 °C and 0.03 at 750 °C, when the melt was an equimolar mixture of lithium-, sodium-, and potassium carbonate [31]. Large lithium content and high temperature reduced the $MgCO_3$ content in the melt, favoring the MgO(s)-phase. We therefore expect a very small amount of $MgCO_3$ in the molten Li_2CO_3 in the presence of MgO(s). This was also the case when we investigated. Nevertheless, the electrolyte of cell LC–XO has for the conditions used here two chemical components.

However, as long as the solid phase of MgO(s) exists, there is only one *independent* component according to the Gibbs phase rule. The chemical potential of $MgCO_3$(l) is dictated by the equilibrium (19) and the gas pressure. The chemical potential of MgO(s) is $\left(\mu_{MgO,T}(s) = \mu_{MgO,T}^0(s) \right)$. Then, with equilibrium in Eq. (19) and $dp_{CO_2} = 0$, $d\mu_{2,T} = d\mu_{MgCO_3,T} = 0$. This, together with the Gibbs-Duhem relation for the electrolyte, gives ($n_1 d\mu_{1,T} + n_2 d\mu_{2,T} = 0$), $d\mu_{Li_2CO_3,T} = d\mu_{1,T} = -n_2 d\mu_{2,T}/n_1 = 0$. Therefore, the expression for the entropy production will be the same as the entropy production for the one-component system, Eq. (10). This gives the same expression for the Seebeck coefficient of cells LC–XO and LC. What will change, as we shall see, is the value of the transport coefficients.

The same reasoning applies to all the oxides used in the present cell. We shall investigate the oxides MgO(s), CeO_2(s) and $LiAlO_2$(s).

2.3. The Seebeck coefficient of cells LC and LC–XO

We add the contribution from the five subsystems to the Seebeck coefficient for the cells LC and LC–XO, see Eq. (2). We choose the cation frame of reference for the electrolyte and add Eqs. (3), (9) and (13). At reversible conditions, the choice of frame of reference

for the mass fluxes will not have an impact on the expression for the potential drop across the surface. The result is:

$$\alpha_S = \frac{\Delta\phi}{(T^{s,c} - T^{s,a})}$$

$$= -\frac{1}{F}\left[\frac{1}{2}S^0_{CO_2} + \frac{1}{4}S^0_{O_2} - \frac{R}{2}\ln p^u_{CO_2} - \frac{R}{4}\ln p^u_{O_2} - \left(\frac{1}{2}S^*_{CO_3^{2-}} - S^*_{e,Au}\right)\right] \quad (20)$$

where we assumed ideal gas and used the relation $S_j = S^0_j + \ln p^u_j$ for the entropies of the gases. In the Eq. above p^u_j is the fraction of the partial pressure and the standard pressure p^0 of component j and S^0_j is the partial molar entropy of component j at temperature T and standard pressure p^0. The entropies and the transported entropies are generally functions of temperature. In the experiments, we keep the average temperature constant and use $\Delta T < 20\,°C$ to avoid temperature corrections. The entropies of the components vary less than 1 % with a 20 degree temperature variation, which is negligible compared to the experimental accuracy. From Eq. (20), and known values of the entropies, the gas partial pressures and the transported entropy of the electron in gold we can calculate the transported entropy of the carbonate ion. We do this in Sections 4.2 and 4.3. A positive $\Delta\phi$ means that the system produces work from the temperature difference between the electrode surfaces, or that heat flows from the high temperature to the low temperature. In this situation, the temperature difference $\Delta T = T^{s,c} - T^{s,a}$ is negative and consequently the Seebeck coefficient is negative for a system that produces work.

From Eq. (20), we can predict the pressure variation of the Seebeck coefficient. For a fixed value of the oxygen pressure, we have:

$$\left(\frac{d\alpha_S}{d\ln p^u_{CO_2}}\right)_{p^u_{O_2}} = \frac{R}{2F} = 0.043\,mV\,K^{-1} \quad (21)$$

3. Experimental

An experimental routine was made to establish the measurement procedure, and to learn about the effect on the transported entropy of carbonate ion in a dispersion. As external agents were added MgO, CeO$_2$ and LiAlO$_2$.

3.1. Materials

Lithium carbonate (Li$_2$CO$_3$) with purity > 99 %, magnesium oxide (MgO) with purity > 99 %, cerium oxide (CeO$_2$) with purity > 99.9 % and lithium aluminate (LiAlO$_2$, lot number: 21804PRV) were acquired from Sigma Aldrich. Chemicals were used without further purification. The specific surface areas of all oxides are given in Table 1.

Pre-made gas mixtures of oxygen and carbon dioxide were obtained from Yara Praxair. Three gas mixtures were used containing 66 % CO$_2$ and 34 % O$_2$, 20 % CO$_2$ and 33 % O$_2$, 7.3 % CO$_2$ and 33 % O$_2$, the rest was He(g). Experiments were performed in a controlled atmosphere of N$_2$(g) of purity $\geq$ 99.999%. The gas mixtures

Table 1
The Seebeck coefficient (α_S) and the transported entropy of the carbonate ion. The uncertainty in the calculated result stems from independent measurements. XO is the added oxide in cell LC-XO and the surface area is determined by BET analysis.

Cell	α_S mV K^{-1}	$S^*_{CO_3^{2-}}$ J K^{-1} mol^{-1}	XO surface area m^2 g^{-1}
LC	-0.88 ± 0.06	232 ± 12	-
LC-MgO	-1.04 ± 0.02	201 ± 4	120
LC-CeO$_2$	-1.05 ± 0.02	200 ± 4	4
LC-LiAlO$_2$	-1.00 ± 0.02	209 ± 4	1

was exposed to 1 bar pressure in the surroundings, meaning that the total pressure in the cell (the sum of the partial pressures) was constant and always equal to 1 bar.

Gold was obtained from K.A. Rasmussen, Norway. Alumina tubes and crucibles were acquired from MTC Haldenwanger, Germany.

3.2. Apparatus

All experiments were performed in a standard laboratory vertical tubular furnace [32]. The cell, shown in detail in Fig. 1b, consisted of an Al$_2$O$_3$ crucible, with electrodes immersed in a molten carbonate electrolyte. Each gold electrode was inserted into the center bore (diameter 2.3 mm) of a 5-bore Al$_2$O$_3$ tube and the gold sheet was point-welded to the wire. The thermocouple (Pt-Pt10%Rh) was inserted into two of the other holes (diameter 0.75 mm) and the junction was positioned as near as possible to the gold sheet. Gas was supplied through the bores of the ceramic tube. The temperatures and cell emf were recorded every third second by a data acquisition unit (Agilent, 34972A).

3.3. Procedure

The electrolyte was either pure lithium carbonate or a dispersion electrolyte of Li$_2$CO$_3$ and one of the oxides MgO, CeO$_2$ or LiAlO$_2$. For all dispersions, the volume fraction of the liquid phase was 0.62. The dispersion electrolytes were prepared by mixing the Li$_2$CO$_3$ with the oxide powder by hand in a mortar. The lithium carbonate or the mixture were pre-heated more than 48 hours at 200 °C in a muffle furnace. After drying, the electrolyte was melted under nitrogen atmosphere at 750 °C in the vertical tube furnace and kept at this temperature for at least 48 hours to ensure stable conditions. Next, the gas mixture (in most cases with the composition 66 % CO$_2$ and 34 % O$_2$) was passed through the 5-bore ceramic tube for at least 5 hours before the experiment started. At the start of each experiment, we adjusted the gas flow rate to give stable measurements. A slow flow rate, adapted for good gas-metal-electrolyte contact was used. With SEM-imaging, we visually inspected the solidified electrolyte of cell LC-MgO. These pictures showed homogeneously distributed particles of grain size around 1-2 μm.

The experiment started when the temperatures and the electric potential were stable. A temperature difference (ΔT) was established between the electrodes by positioning them at different heights in the crucible. The average cell temperature was kept at 750 °C and the temperature difference was always smaller than 20 °C, to avoid the need for temperature corrections in the Seebeck coefficient. The electromotive force between the electrodes was measured as a function of the temperature difference, by gradually first increasing and then decreasing the temperature difference, see Figs. 3 and 4. After an equilibration period of 10-20 min, the cell was again stable, and a measurement with a new temperature difference was done. Recordings were made over time to make sure that the situation was stable, and to eliminate effects of minor instabilities or drift due to voltage fluctuations in the mains. The technique demonstrated in these figures was used to obtain the Seebeck coefficient.

From Figs. 3 and 4, we see that the presence of MgO has a certain stabilizing effect on the voltage recordings. The voltage fluctuation is larger in the first case giving a higher uncertainty compared to the cases when inorganic powder was added. Adding particles to the liquid increase the effective viscosity and prevents convection, resulting in more stable conditions.

We estimated the accuracy (a double standard deviation) from repeated measurements. For cell LC, the Seebeck coefficient was determined for three different gas flows (i.e. different outlet pressures from the gas bottle). This gave a double standard deviation of ± 0.06 mV K^{-1}. For cell LC-XO one series of measurements
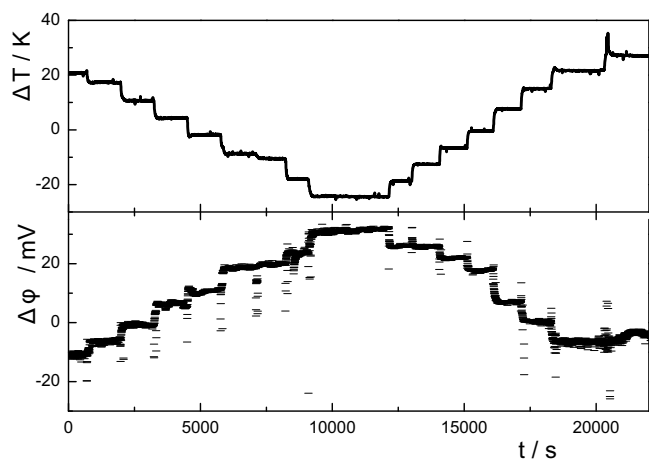
Fig. 3. The measured potential difference ($\Delta\phi$) that follow from variations in the temperature difference (ΔT) as a function of time, in the cell LC. The electrodes were of gold, the average temperature was 750 °C, $p_{CO_2}^u = 0.66$ and $p_{O_2}^u = 0.34$.

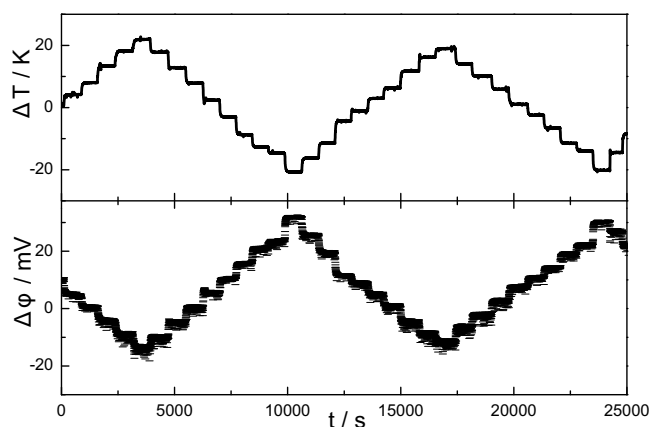**Fig. 4.** The measured potential difference ($\Delta\phi$) and the measured temperature difference (ΔT), c.f. 3, as a function of time for the cell LC-MgO. The electrodes were of gold, the average temperature was 750 °C and $p_{CO_2}^u = 0.66$ and $p_{O_2}^u = 0.34$.
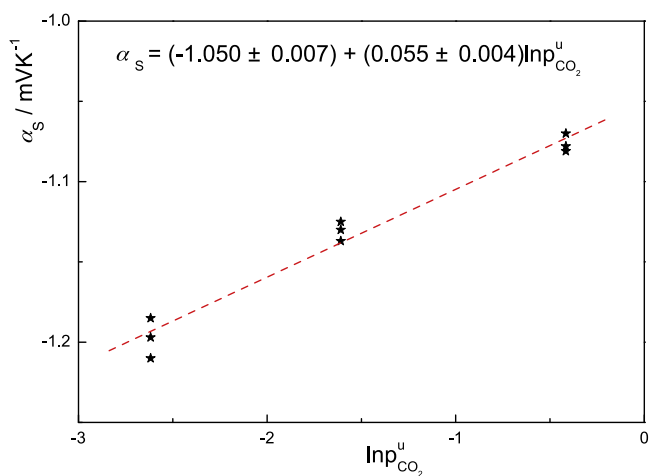

Fig. 5. The Seebeck coefficient for cell LC-MgO as a function of the partial pressure of CO_2, keeping the partial pressure of oxygen constant at 0.33 bar. The electrodes were of gold and the average temperature was 750 °C. The line represents the linear regression.

was reproduced three times, replacing the electrolyte between each experiment. The uncertainty, ± 0.02 mV K^{-1}, was larger than the double standard deviation from linear regression.

In a parallel study, we used also platinum as electrode material [33]. Within the accuracy of the experiment, the two metals gave the same Seebeck coefficient.

3.4. Solubility of magnesium oxide in lithium carbonate with carbondioxide present

We did an independent measurement to determine the solubility of magnesium oxide in lithium carbonate when carbon dioxide was present, see Eq. (19). Pellets of magnesium oxide was added to the lithium carbonate. The gas was supplied at the bottom of the crucible, bubbling over the pellets in contact with lithium carbonate. Samples were collected from the molten phase and analysed for magnesium content (ICP-MS). As reference, we took a sample from the molten lithium carbonate when no magnesium oxide was present. This test confirmed that magnesium oxide is only slightly soluble in lithium carbonate at our conditions, increasing from 0.007 to 0.013 wt%.

4. Results and discussion

4.1. The Seebeck coefficient determination

Figs. 6 and 7 give the emf plotted vs the temperature difference between the electrodes for cells LC and LC-XO with MgO(s) and CeO$_2$(s). The values are averages of values measured over a period in time when the potential was stable. We found the Seebeck coefficients (α_S, see Eq. (2)) as the slopes of these and similar plots. The coefficients obtained in this manner are given in Table 1.

The lines in Figs. 6 and 7 do not cross the origin, meaning that there is a bias potential between the electrodes. The value of the Seebeck coefficient is, however, not affected by any stable, systematic error in the absolute potential. Janz and Saegusa [28] reported stable bias potentials of the order ± 5 mV after an initial aging period for an O$_2$/Au electrode in molten carbonates at 600 °C. Borucka and Sugiyama [29] reported the time stability to be within ± 2 mV for the equilibrium potentials of O$_2$/CO$_2$/Au electrodes in molten carbonates. In our experiments, the thermocouples were positioned close to, but not at the electrode surface. A systematic difference between the *measured* and *actual* surface temperature
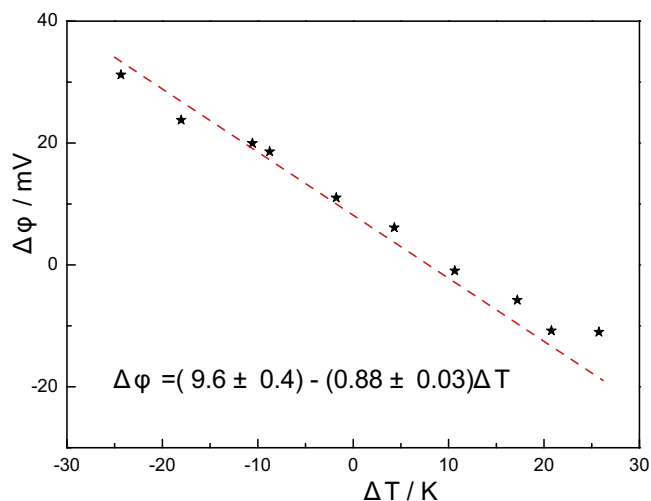

Fig. 6. The measured potential difference ($\Delta\phi$) as a function of the temperature difference between the electrodes (ΔT) in cell LC. The electrodes were of gold, the average temperature was 750 °C, $p_{CO_2}^u = 0.66$ and $p_{O_2}^u = 0.34$.
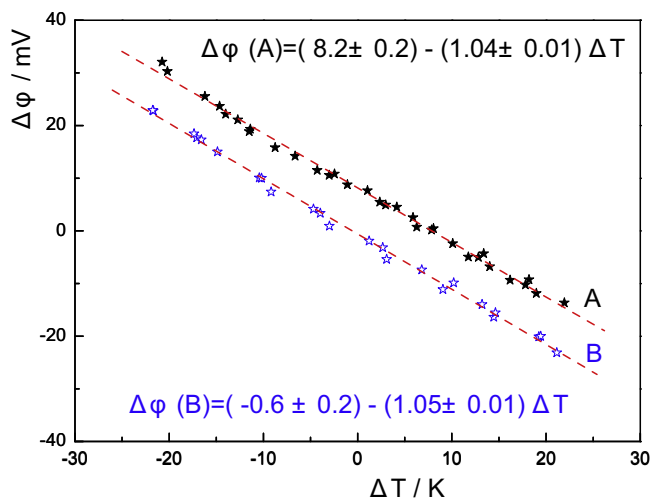
Fig. 7. The measured potential difference ($\Delta\phi$) as a function of the temperature difference between the electrodes (ΔT) in cell LC-MgO (A) and for cell LC-CeO$_2$ (B). The electrodes were of gold, the average temperature was 750 °C, $p_{CO_2}^u = 0.66$ and $p_{O_2}^u = 0.34$.

Table 2
Thermodynamic and transported entropies at 750 °C. The thermodynamic entropy applies to a bulk liquid. The transported entropy of lithium is found from Eq. (20) with measured values of the Seebeck coefficient.

cell	$S_{Li_2CO_3}$ $J K^{-1} mol^{-1}$	$S^*_{CO_3^{2-}}$ $J K^{-1} mol^{-1}$	$S^*_{Li^{2+}}$ $J K^{-1} mol^{-1}$
LC	309	232 ± 12	39 ± 12
LC-LiAlO2	287[*]	209 ± 4	39[*]

[*] Estimated

may therefore also arise. This may give a systematic error in the Seebeck-coefficient, as the real temperature difference differs from the measured. Based on the observed Seebeck coefficients, 1 mV off-set corresponds to a constant temperature off-set bias of 1 K. This is around 2 % of the overall temperature range. Also, any small variation in gas concentration or surface concentration is represented by the bias potential and does not affect the results for the Seebeck coefficient. Aging of electrodes could cause a drift, but this was not observed.

As shown by Eq. (21), the slope of a plot of the Seebeck coefficient versus the $\ln p_{CO_2}^u$ is 0.043 mV K^{-1} for the electrode reaction in Eq. (1). The plot shown in Fig. 5 confirms the expected theoretical slope of Eq.21, within the accuracy of the experiment and thus the electrode reaction. This allowed us to use Eq. (20) to analyse the contributions to the Seebeck coefficient and to calculate the transported entropy of the carbonate ion (see Sections 4.2 and 4.3).

4.2. The transported entropy of the carbonate ion in pure lithium carbonate

From Eq. (20), we calculated the transported entropy of the carbonate ion. Standard entropies of the CO$_2$(g), O$_2$(g) and lithium carbonate at 750 °C were 271, 244 and 309 J K^{-1} mol^{-1} (HSC chemistry). The transported entropy of the electron in the gold conductor was 0.4 J K^{-1} mol^{-1} [34]. With this, we calculated the transported entropy of the carbonate ion for the cells LC and LC-XO, see Table 1 for results. The largest value was obtained for pure molten lithium carbonate, 232 ± 12 J K^{-1} mol^{-1}.

The transported entropy is an energy carried along with the charge carrier, an energy of a type that draws from order-disorder transitions as the charge is carried along. The carbonate ion has rotational degrees of freedom in the carbonate melt which can be influenced by the surroundings [35]. This property could therefore be connected to a high value of the transported entropy.

4.3. The transported entropy of the carbonate ion in a dispersion

We see from Table 1 that the transported entropy of the carbonate ion decreases substantially when solid MgO or another oxide is added to the electrolyte. The smaller transported entropy is compatible with a larger value of the Seebeck coefficient. From the point

of view of applications, a smaller value is therefore most interesting. The factors that affect the variation are therefore of interest.

It is clear from the theoretical derivations, that the sole reason for the variation in the transported entropy of carbonate ion comes from the fact that the liquid electrolyte is included in a dispersion. The fact that gold and platinum electrodes gave the same Seebeck-coefficient, see [33], excludes an impact of the electrode material. The electrode reaction is the same in the presence and absence of the oxide in the electrolyte. The electrode reaction shows furthermore the expected dependence on the partial pressure of carbon dioxide. From the BET surface of all oxides (see Table 1) and SEM imaging, it seems clear that the molten lithium carbonate is not in a bulk state inside the dispersions.

Given that the presence of LiAlO$_2$(s), but not CeO$_2$(s), alters the symmetry of the carbonate ion [25,26], one would expect a variation in the transported entropy of the carbonate ion between the two dispersions. The results 200 and 209 J K^{-1} mol^{-1} differ within the uncertainty in the results, but barely so. If the ability to polarize leads to an increasing value, the results indicate that LiAlO$_2$ has the highest polarizing ability of the oxides used. Also, LiAlO$_2$ had the smallest BET surface area, see Table 1.

Blinov et al. [36] calculated the transported entropy of lead ion in mixtures with alkali chlorides, and found a value, affected by the field strength of the alkali metal, or the polarizing power. The transported entropy of lead ion was larger in the presence of Li$^+$ than of Cs$^+$. This variation can be said to support our finding. The more polarizing the surroundings are, the larger is the number of states to explore upon transport, and the higher becomes the value of transported entropy.

Capillary effects are expected in the dense dispersions. Mizuhata et.al. [37] found that the enthalpy of melting of Li$_2$CO$_3$ was reduced with 50-80 % of the normal value by including the salt in a dispersion with LiAlO$_2$. Reductions in the freezing point could also be seen [37]. The reductions were dependent on the ratio of molten carbonate and the total surface area of the solid phase. A lowering of the enthalpy of melting, indicates that the entropy of the liquid phase becomes lower. The value of the entropy of the salt in the porous material will therefore differ from the bulk value. The relation in Eq. (18) can be used used to argue why $S^*_{CO_3^{2-}}$ obtains a reduction. Janz and co-workers [38] reported an enthalpy of melting of 44.8 kJ mol−1 and the melting point 726 °C for pure Li$_2$CO$_3$. For a 50 % reduction in the enthalpy of melting for the pure salt, this gives a reduction of 22 J K^{-1} mol^{-1} in the entropy at 750 °C. The observed reduction is from 232 to 209 J K^{-1} mol^{-1} or 23 J K^{-1} mol^{-1}. The lowering in the entropy of the salt, compatible with a more ordered structure inside the dispersion, can explain the lowering in the transported entropy of the carbonate ion seen in Table 2. The numbers are, however, uncertain and there could also be an increase in the transported entropy of the lithium ion.

The values from the BET experiments show that addition of the solid phase creates extra surfaces in the system, varying with the grain size of the powders added. Such added surface is likely to have an impact on the electrical and thermal conductivity of the melt, properties which play an important role in the figure of merit. Introducing the electrically non-conducting solid phase to

the system lowers the electrical conductivity. Mizuhata et. al. [37] reported electrical conductivities increasing exponentially with the volume fraction of the molten carbonate. A non-linear increase indicates that the surface, introduced with the particles, give a contribution to the conductivity. The solid phase will most likely also affect the thermal conductivity. At the end, a possible successful system for thermoelectric power generation do also depend on other concerns such as safety and cost.

5. Conclusions and perspectives

We have measured for the first time the Seebeck coefficient of an electrochemical cell with gas electrodes reversible to the carbonate ion, and a molten lithium carbonate in the absence and presence of an inorganic oxide. In the pure electrolyte, the coefficient was $0.88\,mV\,K^{-1}$, rising to $1.04\,mV\,K^{-1}$ for the dispersion. The transported entropy of carbonate ion varied from 232 to $200\,J\,K^{-1}\,mol^{-1}$, possibly due to a decreasing polarizing environment and an ordering of the salt in the dispersion of the oxide.

The cheap materials, and the potential to further increase the Seebeck coefficient, in combination with a good overall electric conductivity, make the material types suitable candidates for electrochemical energy conversion in the future. In this context more systematic experiments are needed to optimize conditions for conversion.

Acknowledgment

References

[1] Jacobsson Staffan, Anna Johnson, The diffusion of renewable energy technology: an analytical framework and key issues for research, Energy Policy 28 (2000) 625–640.
[2] N.L. Panwar, S.C. Kaushik, Surendra Kothari, Role of renewable energy sources in environmental protection, Renewable and Sustainable Energy Reviews 15 (2011) 1513–1524.
[3] Fernando deLlando-Paz, Anxo Calvo-Silvosa, Susana Iglesias Antelo, Isabel Soares, The European low-carbon mix for 2030: The role of renewable energy sources in an environmentally and socially efficient approach, Renewable and Sustainable Energy Reviews 48 (2015) 49–61.
[4] L.E. Bell, Cooling, heating, generating power, and recovering waste heat with thermoelectric systems, Science 321 (2008) 1457–1461.
[5] Joseph R. Sootsman, Duck Young Chung, Mercouri G. Kanatzidis, New and old concepts in thermoelectric materials, Angew. Chem. Int. Ed. 48 (2009) 8616–8639.
[6] M. Zebarjadi, K. Esfarjani, M.S. Dresselhaus, Z.F. Ren, G. Chen, Perspectives on thermoelectrics: from fundamentals to device applications, Energy and Environmental Science 5 (2012) 5147-.
[7] Shannon K. Yee, Saniya LeBlanc, Kenneth E. Goodson, Chris Dames, $ per W metrics for thermoelectric power generation: beyond ZT, Energy Environ. Sci. 6 (9) (2013) 2561–2571.
[8] Saniya LeBlanc, Shannon K. Yee, Matthew L. Scullin, Chris Dames, Kenneth E. Goodson, Material and manufacturing cost considerations for thermoelectrics, Renewable and Sustainable Energy Reviews 32 (2014) 313–327.
[9] T.C. Harman, J.M. Honig, Thermoelectric and Thermomagnetic Effects and Applications, McGraw-Hill, New York, 1967.
[10] J.N. Agar, in: P. Delahay (Ed.), Advances in Electrochemistry and Electrochemical Engineering, volume 3, chapter Thermogalvanic cells, Interscience, New York, 1963.
[11] S.R. de Groot, P. Mazur, Non-Equilibrium Thermodynamics, London, Dover, 1984.
[12] K.S. Førland, T. Førland, S. Kjelstrup, Irreversible Thermodynamics. Theory and Application, 3rd edition, Tapir, Trondheim, Norway, 2001.
[13] A. Bentien, S. Johnsen, G.K.H. Madsen, B.B. Iversen, F. Steglich, Colossal Seebeck coefficient in stronlgy correlated semiconductor $FeSb_2$, European Physics Letters 80 (2007), 17008-.
[14] Hiromichi Ohta, SungWng Kim, Yoriko Mune, Teruyasu Mizoguchi, Kenji Nomura, Shingo Ohta, Takashi Nomura, Yuki Nakanishi, Yuichi Ikuharaand, Masahiro Hirano, Hideo Hosono, Kunihito Koumoto, Giant thermoelectric Seebeck coefficient of a two-dimensional electron gas in $SrTiO_3$, Nat. Mater. 6 (2007) 129–134.
[15] Kyu Hyoung Lee, Yoriko Mune, Hiromichi Ohta, Kunihito Koumoto, Thermal Stability of Giant Thermoelectric Seebeck Coefficient for $SrTiO_3/SrTi_{0.8}Nb_{0.2}O_3$ Superlattices at 900 K, Applied Physics Express 1 (1) (2008) 015007–015008.
[16] M. Bonetti, S. Nakamae, M. Roger, P. Guenoun, Hughe Seebeck coefficients in nonaqueous electrolytes., J. Chem. Phys. 134 (2011), 114513-.
[17] B. Flem, Q. Xu, S. Kjelstrup, Å. Sterten, Thermoelectric powers of cells with NaF-AlF_3-Al_2O_3 melts, J. Non-Equilib. Thermodyn. 26 (2001) 125–151.
[18] T. Jacobsen, G.H.J. Broers, Single Electrode Heat Effects I. Peltier Heats of Gas Electrodes in Carbonate Paste Electrolytes, J. Electrochem. Soc. 124 (1977) 207–210.
[19] Bruno B. Sales, Odne S. Burheim, Slawomir Porada, Volker Presser, Cees J.N. Buisman, Hubertus V.M. Hamelers, Extraction of energy from small thermal differences near room temperature using capacitive membrane technology, Environmental Science & Technology Letters 1 (9) (2014) 356–360.
[20] Marit Takla, Odne S. Burheim, Leiv Kolbeinsen, Signe Kjelstrup, A solid state thermoelectric power generator prototype designed to recover radiant waste heat, in: Maria D. Salazar-Villalpando, Neale R. Neelameggham, Donna Post Guillen, Soobhankar Pati, Gregory K. Krumdick (Eds.), Energy Technology 2012: Carbon Dioxide Management and Other Technologies, March 2012.
[21] Anders Schei, Johan Kr. Tuset, Halvard Tveit, Production of High Silicon Alloys. Tapir, Trondheim, Norway, 1998.
[22] Nils Eivind Kamfjord, Mass and Energy Balances of the Silicon Process. PhD thesis, NTNU, Trondheim, 2012.
[23] M. Takla, N. Kamfjord, H. Tveit, S. Kjelstrup, Energy and exergy analysis of the silicon production process, Energy 58 (2013) 138–146.
[24] S. Kjelstrup, D. Bedeaux, Non-equilibrium thermodynamics of heterogeneous systems, World Scientific, Singapore, 2008.
[25] M. Mizuhata, T. Ohta, S. Deki, Polarized Raman Spectra of Molten Carbonates Influenced by the Surface Acidity of the Coexisiting Inorganic Powder, Electrochemistry 77 (2009) 721–724.
[26] Minoru Mizuhata, Toshifumi Ohashi, Alexis Bienvenu Béléké, Electrical conductivity and related properties of molten carbonates coexisting with ceria-based oxide powder for hybrid electrolyte, International Journal of Hydrogen Energy 37 (2012) 19407–19416.
[27] Jong-Wan Kim, Yong-Deuk Lee, Hae-Geon Lee, Decomposition of li 2 co 3 by interaction with sio 2 in mold flux of steel continuous casting, ISIJ international 44 (2) (2004) 334–341.
[28] G.J. Janz, F. Saegusa, The oxygen electrode in fused electrolytes, Electrochimica Acta 7 (1962) 393–398.
[29] Alina Borucka, C.M. Sugiyama, Thermodynamic evaluation of the $O_2/CO_2/Au$ gas electrode in molten alkali carbonates, Electrochimica Acta 13 (1968) 1887–1897.
[30] S.Kjelstrup Ratkje, H. Rajabu, Transference coefficients and transference numbers in molten salt mixtures relevant for the aluminium electrolysis, Electrochim. Acta 38 (1993) 415–423.
[31] P.F. van Velden, Equilibrium between (Li,Na,K,Mg)-Carbonate Melt, Gaseous CO_2 and MgO, Trans Faraday Soc. 63 (1967) 175–184.
[32] Ketil Motzfeldt, High Temperature Experiments in Chemistry and Materials Science, John Wiley, UK, 2013.
[33] X. Kang, M.T. Borset, O.S. Burheim, G.M. Haarberg, Q. Xu, S. Kjelstrup, Seebeck coefficients of cells with molten carbonates relevant for the metallurgical industry, Electrochimica Acta 182 (2015) 342–350.
[34] C.Y. Ho, R.H. Bogaard, T.C. Chi, T.N. Havill, H.M. James, Thermoelectric power of selected metals and binary alloy systems, Thermochimica Acta 218 (1993) 29–56.
[35] J.T.W.M. Tissen, G.J.M. Janssen, Molecular-dynamics simulation of molten alkali carbonates, Molecular Physics 71 (1990) 413–426.
[36] V. Blinov, S. Kjelstrup, D. Bedeaux, V.S. Sharivker, The role of the transported entropy of lead in partially thermostatted and adiabatic cells, J. Electrochem. Soc. 148 (2001) 364–371.
[37] Mizuhata Minoru, Yasuyuki Harada, Guem ju Cha, Alexis Bienvenu Béléké, Shigehito Deki, Physicochemical Properties of Molten Alkali Metal Carbonates Coexisting with Inorganic Powder, J. Electrochem. Soc. 5 (2004) E179–E185.
[38] G.J. Janz, E. Neuenschwander, F.J. Kelly, High-temperature heat content and related properties for Li_2CO_3, Na_2CO_3, K_2CO_3 and the ternary eutectic mixture, Trans. Faraday Soc. 59 (1963) 841–845.